ORIGINAL PAPER

Microscopic Investigation of Rock Direct Tensile Failure Based on Statistical Analysis of Acoustic Emission Waveforms

Zhenghu Zhang[1,2] · Ke Ma[1,2] · Hua Li[3] · Zhiliang He[4]

Abstract

Tensile strength is a vital mechanical property of rock and the deformation and failure process of rock under tension is of much significance in rock mechanics and engineering. In this study, a micro analysis on rock direct tensile failure was made based on the newly introduced quantitative analysis of acoustic emission (AE) waveforms. Direct tensile tests of common rocks were carried out, accompanied by real-time AE monitoring. The spatial and temporal distributions of AE signals were studied over the whole loading process. Distribution and evolution laws of dominant frequencies of AE waveforms with normalized applied stress were statistically analyzed. The statistical relationship between the energy ratios of AE waveforms distributed in low and high dominant frequency bands (L-type and H-type waveforms) and peak strengths of rock specimens was built. Microstructural observations with SEM were further conducted. Results show that the dispersion degree of rock tensile strength corresponds to the complexity of mineral composition. Initial release moments of L-type waveforms appeared earlier than H-type waveforms. L-type waveforms of the same proportion carry more energy compared to H-type waveforms in rock subjected to tension. There is an overall downward trend for peak strength of rock specimens with the increasing energy ratios of L-type waveforms. The tensile strength of rock obtained by fitting in this study is smaller than that obtained by averaging. There exist micro shear fractures during the macro tensile failure process of rock according to the microstructural observations with SEM. The peak strength corresponding to the case that L-type waveforms (or micro tensile failures) account for 100% can be considered as the "ideal" tensile strength from the microscopic perspective. The determined tensile strength by fitting can be used as a conservative design parameter for rock engineering.

Highlights

- Statistical relationship between energy ratios of AE waveforms distributed in low and high dominant frequency bands and peak strengths of rocks under tension is built.
- There exist micro shear fractures during the macro tensile failure process of rock.

- Peak strength in the case that L-type waveforms (or micro tensile failures) reach 100% can be considered as the "ideal" tensile strength.
- The determined tensile strength by fitting can be used as a conservative design parameter for rock engineering.

✉ Ke Ma
mark1983@dlut.edu.cn

1   Centre for Rock Instability and Seismicity Research, School of Civil Engineering, Dalian University of Technology, Dalian 116024, China

2   State Key Laboratory of the Coastal and Offshore Engineering, Dalian University of Technology, Dalian 116024, China

3   College of Water Resource and Hydropower, Sichuan University, Chengdu 610065, China

4   School of Environment and Resource, Southwest University of Science and Technology, Mianyang 621010, China

1 Introduction

In addition to compression and shear strength, tensile strength is an indispensable property to evaluate the stability and reliability of rock structures (Hobbs 1967; ISRM 1978). The tensile strength of rock refers to the maximum tensile stress that a rock can withstand when it reaches failure subjected to tension. The tensile strength of rock is far less than its corresponding compression strength (Diederichs and Kaiser 1999; Dan et al. 2013; Zhang et al. 2020). Rock failure often originates from the initiation and propagation of a tensile crack in tunnel construction, rock slope excavation, rock drilling and blasting engineering (Goodman 1989). Deformation and failure of rock under tensile load is a basic scientific issue in rock mechanics and geotechnical engineering. Tensile strength is a vital mechanical parameter for determining the bearing capacity of rocks. Therefore, the deformation and failure process of rock subjected to tension is of great significance to evaluate the stability of rock structures in many fields, e.g., civil engineering, hydraulic engineering, mining and energy engineering.

There are two existing methods for determining the tensile strength of rocks, including the direct tensile test and indirect tensile test (Ishiguro and Nakaya 1985; Fahimifar and Malekpour 2012; Perras and Diederichs 2014). The direct tensile test has a clear physical meaning, which is more consistent with the actual situation of the rock under tension (Wijk et al. 1978). In contrast, indirect Brazilian splitting test cannot achieve pure tensile loading conditions for rock samples because of the special experimental configuration. The direct tensile test has been widely used in a laboratory experiment and engineering practice (e.g., Toutanji et al. 1999; Liao et al.1997; Wu et al. 2018). However, the rock is a natural geological material with a complex internal structure and it contains many cavities, pores and other microstructures, which leads to complex microscopic failure processes and mechanisms of rocks. Even if the rock shows a tensile failure on a macroscopic level, it may contain shear or mixed failure on a microscopic level. Therefore, it is necessary to understand macroscopic tensile failure from a microscopic point of view.

It is very difficult to quantitatively study rock failure, especially microscopic failure. As a common non-destructive testing approach, acoustic emission (AE) technique can be applied to analyze and study the real-time initiation, propagation and coalescence of micro failures in brittle materials because acoustic emission is the transient elastic wave released by micro failures in a material due to a rapid release of strain energy (Karser 1950; Sondergeld and Estey 1981; Shiotani et al. 2001; Cai et al. 2007). Currently,

AE technique has been widely used to investigate the failure process and mechanism of rock subjected to an external load (e.g., Zhou et al. 2016; Zhang and Deng 2020; Du et al. 2020; Liang et al. 2020). There are two main methods, namely parameter-based and waveform-based methods, to analyze AE signals. Parameter-based method, which is characterized by a series of parameters such as AE hit, event and count, is more widely used due to its convenience and efficiency, while waveform-based method is time-consuming with high equipment requirements (Grosse and Ohtsu 2008). With the rapid development of sensors and computational processors, micro failure process and mechanism of rock have recently begun to be studied based on the dominant frequency feature of AE waveforms (Shiotani et al. 2001; Aker et al. 2014; Zhang et al. 2020). There are two dominant frequency concentration bands in different rocks under different loading conditions (He et al. 2010; Li et al. 2017). In particular, Li et al. (2017) further found that the waveforms with high dominant frequency (H-type waveforms) are produced by micro-shear failure and the waveforms with low dominant frequency (L-type waveforms) are released by micro-tensile failure. Subsequently, statistical analyses of dominant frequency characteristics of AE signals were applied to investigate the failure mechanism of jointed and intact rocks (Zhang et al. 2018), moisture-induced softening mechanism (Huang et al. 2019) and determination of the crack classification criterion in AE parameter analysis (Zhang et al. 2020). These above-mentioned studies based on statistical analyses of dominant frequency characteristics of AE waveforms provide a new perspective to study micro failure types in rock, which will be adopted in this study.

The objective of this study is to investigate the evolution process of microcracks in rock under tension using the newly introduced quantitative analysis of acoustic emission (AE) waveforms. First, direct tensile tests of common rocks were conducted to obtain peak strengths of rock under tension, accompanied by real-time AE monitoring. Subsequently, dominant frequencies of AE signals were acquired and then number and energy ratios of AE waveforms distributed in different dominant frequency bands with the applied stress were statistically analyzed. Then the relationship between the energy ratios of L-type waveforms and peak strengths of a group of rock samples was established. Finally, the tensile failure process of rock was discussed from a microscopic perspective.
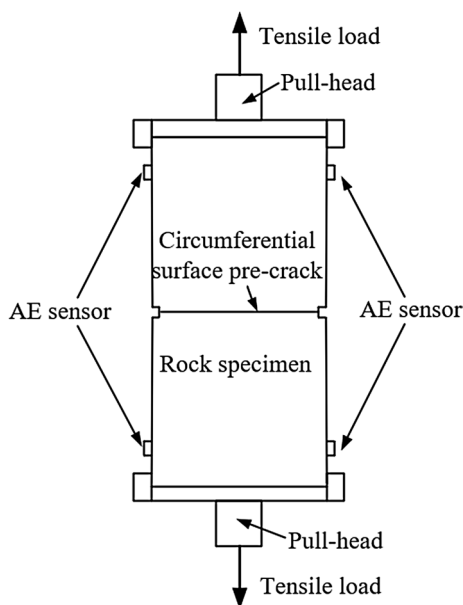
Fig. 1 Schematic diagram of rock specimen and acoustic emission monitoring

Table 1 Physical and mechanical parameters of rocks

Rock type	Density (10^3 kg/m^3)	Porosity (%)	Water content (%)	UCS (MPa)	Young's modulus (GPa)
Granite	2.62	1.08	0.05	92.76	24.04
Basalt	2.92	0.23	0.07	265.80	72.10
Marble	2.68	0.21	0.01	41.00	22.84

2 Experimental Setup

2.1 Specimen Preparation

Rock specimens with a height of 100 mm and a diameter of 50 mm were fabricated for direct tensile tests. To eliminate the impact of unknown large defects and guarantee a good experimental effect, a circumferential surface pre-crack with a width of 2 mm and a depth of 3 mm was prepared in the middle cross-section of each sample (see Fig. 1). Common rocks, including granite, basalt and marble, were used in this study. Granite samples were taken from the underground powerhouse of Dagangshan Hydropower Station in Dadu River Basin, located in Shimian County, Sichuan Province, China. The horizontal and vertical buried depths of granite samples are about 340 and 450 m. Basalt was sampled in the underground powerhouse of Xiluodu Hydropower Station in the Jinsha River Basin, located in the border area of Leibo County in Sichuan Province and Yongshan County in Yunnan Province. The horizontal and vertical buried depths of basalt are approximately 350 and 400 m, respectively. The marble was sampled at a marble open-pit mine located in Baoxing County, Sichuan Province, China.

In total, there are five granite, five basalt and eight marble specimens for experiments, numbered from G1 to G5, B1 to B5 and M1 to M8, respectively. JGN strong adhesive was used to bond the rock specimen to the test pull-head and each specimen was in a vertical line with the two pull-heads. Then rock specimens with the attached pull-heads were stored at room temperature for one week to guarantee a good connection between the specimen and pull-heads at both ends. The average densities are 2.62, 2.92 and 2.68×10^3 kg/m^3 for granite, basalt and marble, respectively. The average uniaxial compression strengths (UCS) are 92.76, 265.80 and 41 MPa for granite, basalt and marble specimens, while Young's moduli are 24.04, 72.10 and 22.84 GPa, respectively, as listed in Table 1. The average porosity are 1.08%, 0.23% and 0.21% and average water content are 0.05%, 0.07% and 0.01% for granite, basalt and marble specimens (Table 1).

2.2 Experimental Procedure

A rock mechanics testing system (model: MTS 815 Flex Test GT) was applied to carry out direct tensile tests. An acoustic emission acquisition system (model: PCI-2) was used to automatically collect AE signals during the whole loading process. AE signals were monitored by eight Micro30 sensors with a natural frequency of 200 kHz, which were symmetrically distributed on the surface of each specimen about the longitudinal axis, as shown in Fig. 1. Vaseline was utilized between each specimen and AE sensors for good connection.
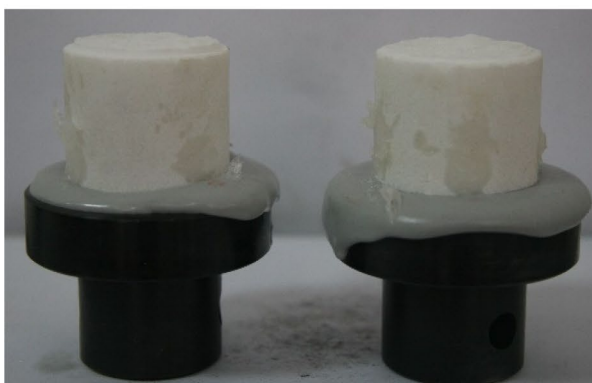
Table 2 Mineral composition of rock

Rock type	Content of minerals (%)						
	Calcite	Quartz	Albite	Pyroxene	Bytownite	Iron oxide	Aluminum phosphate
Granite	–	47	–	–	52	0.5	0.5
Basalt	–	8	66	26	–	–	–
Marble	100	–	–	–	–	–	–
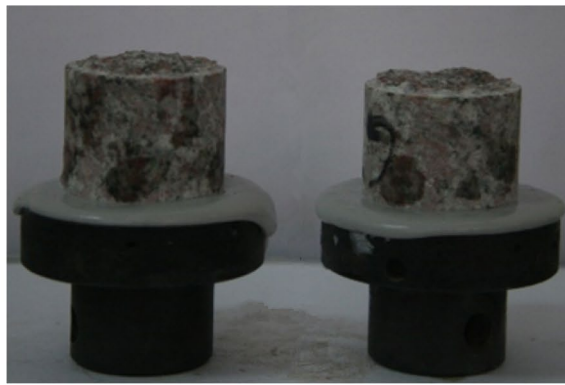
(a)
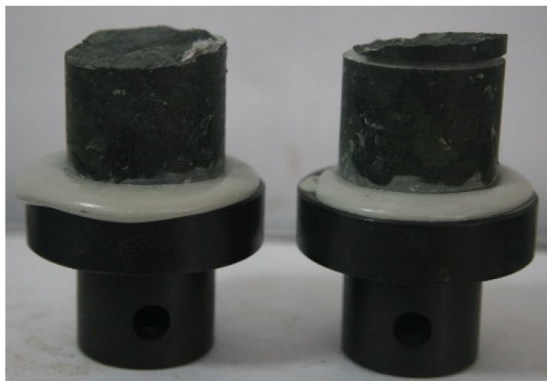
(b)

(c)

Fig. 2 Rock specimens after testing: **a** granite, **b** basalt and **c** marble

Table 3 Tensile strengths of rock specimens

Rock type	Specimen no.	Peak strength (MPa)	Tensile strength (MPa)	
			Mean	Standard deviation
Granite	G1	4.29	4.12	0.49
	G2	3.63		
	G3	4.06		
	G4	3.65		
	G5	4.96		
Basalt	B1	11.92	10.74	2.24
	B2	12.09		
	B3	9.23		
	B4	7.14		
	B5	13.31		
Marble	M1	3.38	3.39	0.13
	M2	3.70		
	M3	3.43		
	M4	3.27		
	M5	3.28		
	M6	3.33		
	M7	3.43		
	M8	3.28		

3 Results and Analysis

3.1 Relationship Between Macro Tensile Properties and Mineral Composition of Rock

A CCD X-ray Single Crystal Diffractometer (Model: Xcalibur E) was used for mineral component analysis. Three samples of each rock type were obtained from different positions for mineral examination. The mineral composition of each rock was determined by averaging the results of three test samples, as shown in Table 2. Granite is mainly constituted by two minerals, i.e., quartz and bytownite (accounting for 99%), and contains a small amount of iron oxide and aluminum phosphate (1%). Basalt mainly consists of three minerals, namely, albite, pyroxene and quartz, which account for 66%, 26% and 8%, respectively. Furthermore, it can be seen from direct observation with the naked eye that there are a few porphyritic textures in basalt samples. Marble is composed of only a single mineral, i.e., calcite. According to the mineral component analysis, marble is more homogeneous and isotropic compared to granite and basalt. The mineral composition and cementation type of the different minerals in basalt are more complicated than granite.

Typical macro failure patterns of granite, basalt and marble specimens after direct tensile testing are shown in Fig. 2. Obviously, the macroscopic tensile failure occurred at or near the middle cross section of each specimen. To be specific, except for the failure of only one basalt specimen that is not completely along the circumferential pre-crack (Fig. 2b), all the failures of granite, marble and basalt specimens occurred at the middle cross-section, i.e., along the circumferential pre-crack. This may be attributed to the more complex mineral composition of basalt compared to marble and granite. Tensile failure may occur at the interfaces of different minerals or pre-existing defects (micro cracks or pores).

The peak strength (σ_{max}) of each rock specimen is the maximum axial force (P_{max}) divided by the area of the middle cross-section of rock specimen (S).

$$\sigma_{max} = \frac{P_{max}}{S}, \tag{1}$$

$$S = \pi \left(\frac{D}{2} - L \right)^2, \tag{2}$$

where σ_{max}, P_{max} and S represents the peak strength of rock, the maximum axial force and the area of the middle cross-section, D and L refer to the diameter of rock specimen and the depth of the circumferential surface pre-crack.

Peak strengths of each specimen were calculated by Eqs. (1) and (2). As listed in Table 3, the peak strength of granite specimens ranges from 3.63 to 4.96 MPa. The range of peak strength of basalt specimens is from 7.14 to 13.31 MPa. The peak strengths of marble specimens range from 3.27 to 3.70 MPa. On average peak strengths of granite, basalt and marble specimens subjected to tension are 4.12, 10.74 and 3.39 MPa, respectively. The dispersion degree of tensile strengths for rocks was analyzed by calculating the standard deviation. The standard deviations of tensile strengths are 0.49, 2.24 and 0.13 MPa for granite, basalt and marble. Obviously, the degree of dispersion from high to bottom corresponds to basalt, granite and marble respectively. After comparing the mineral composition and dispersion degree of tensile strengths for different rocks, it can be found that the discreteness of rock strength is closely related to the mineral composition and microstructure of the rock. Therefore, the dispersion degree of rock tensile strength corresponds well to the complexity of mineral composition and cementation type.
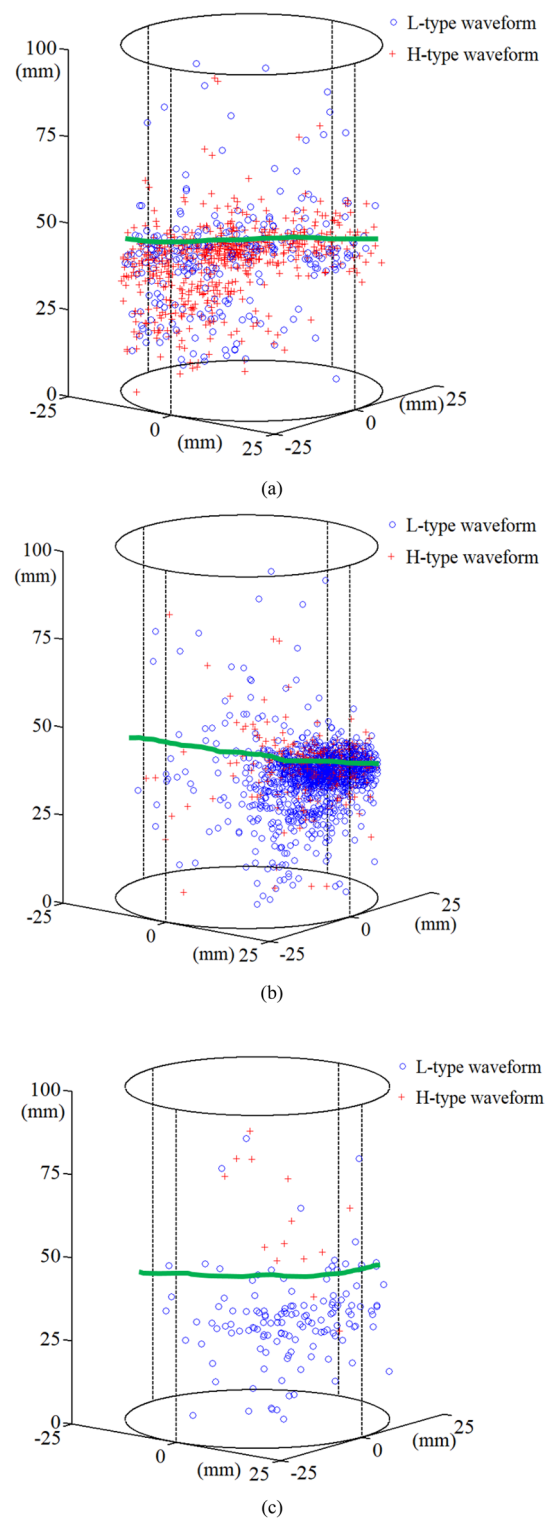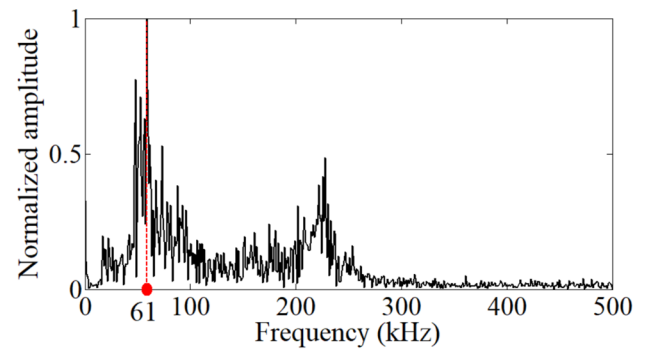

Fig. 3 Representative spatial distribution of L-type and H-type AE waveforms: **a** granite; **b** basalt and **c** marble. Note that black and green lines refer to the specimen boundaries and macroscopic cracks, respectively

(a)

(b)

(c)
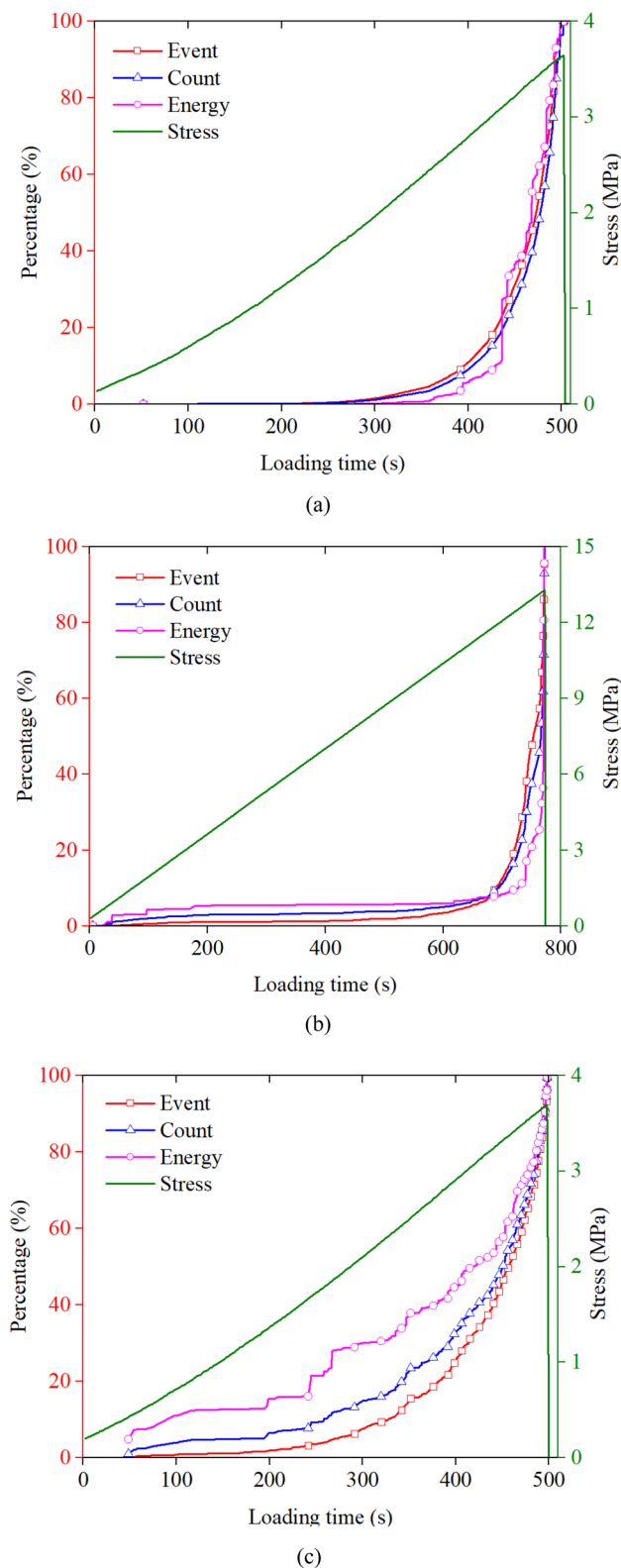
Fig. 4 Typical variation of the normalized ratio of characteristic parameters of rock specimens with the loading time: **a** granite; **b** basalt and **c** marble
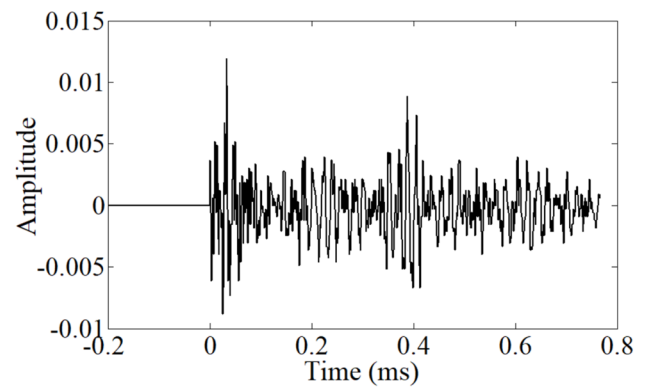
(a)

(b)

Fig. 5 Typical AE waveform and its corresponding spectrum: **a** AE waveform and **b** amplitude spectrum

3.2 Spatial and Temporal Distributions of AE Signals over the Loading Process

Representative spatial distributions of AE waveforms for different types of rock are shown in Fig. 3. Note that black and green lines refer to the specimen boundaries and macroscopic cracks, respectively. Rock specimens show obvious brittle failure. It is found that AE signals are concentrated near the middle cross section of rock specimens, which is basically consistent with macro failure patterns.

AE characteristic parameters can be extracted from AE signals, mainly including hit, event, count, energy, rising time, duration time and maximum amplitude. AE event can represent the total amount and frequency of AE events, and is used to evaluate the activity and location concentration of acoustic emission sources. The AE count is the number of oscillations beyond the threshold value, which can reflect the intensity and frequency of acoustic emission signal. The energy is the area under the signal detection envelope, which is used to characterize the energy or intensity of AE events. In this paper, the three characteristic parameters, including event, count and energy, were used to analyze the evolution law of AE signals. To compare and analyze the evolution law

between different rock samples and different characteristic parameters, three characteristic parameters were normalized. The normalized ratio of characteristic parameters is defined as:

$$\alpha = n/N, \tag{3}$$

where n and N represent the number at a certain time and the total number generated during the whole loading process, respectively.

The cumulative normalized ratios of AE parameters with the increasing loading time are shown in Fig. 4. Although there are local differences between the cumulative curves of AE event, count and energy, the overall trends of the three parameters are similar to the loading time. During the initial loading stage, the normalization ratio of AE characteristic parameters of rock samples is very low, which indicates that the AE events released by rock samples in this stage are very few, and the corresponding count and energy are also very low. At higher stress levels, especially when the stress approaches the peak strength, the normalization ratio of AE characteristic parameters rises sharply and the growth rate increases obviously. This indicates the rock failure is an obviously brittle failure.

3.3 Dominant Frequency Characteristics of AE Signals over the Loading Process

3.3.1 Extraction of Dominant Frequencies of AE Waveforms

Waveform data of AE signals were recorded in real time by the acoustic emission monitoring system. To acquire dominant frequencies of AE waveforms, spectrum analysis was conducted via fast Fourier transform (FFT), which is an effective method to transform AE waveforms in the time domain to the frequency domain. Figure 5 shows a representative AE waveform and its corresponding amplitude spectrum. The dominant frequency, which is defined as the frequency corresponding to the maximum amplitude, was determined in the spectrum. For example, the dominant frequency, marked by a red dot in Fig. 5b, was 61 kHz. To process numerous waveform data efficiently, dominant frequencies were calculated by a batch program written in MATLAB software.

3.3.2 Proportions of AE Waveforms Distributed in Low and High Dominant Frequency Bands

Figure 6 shows distribution characteristics of dominant frequencies of AE waveforms with normalized applied stress in rock samples. Obviously, there are two concentrations of dominant frequency bands, called the low dominant
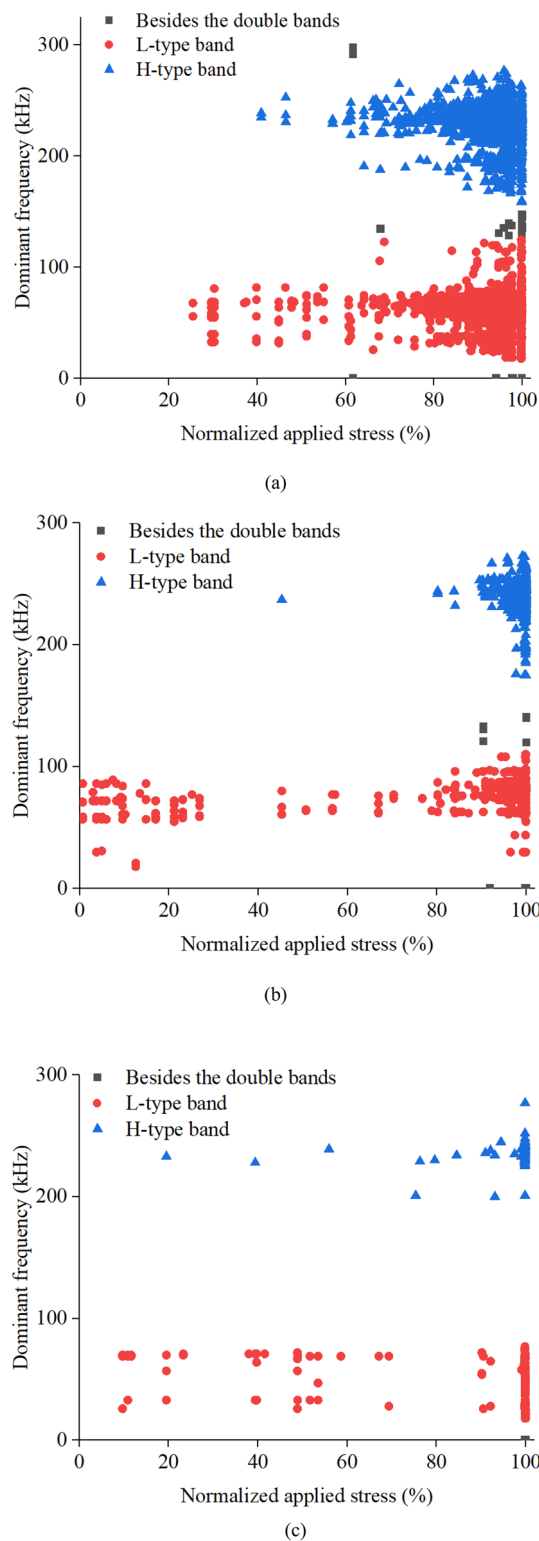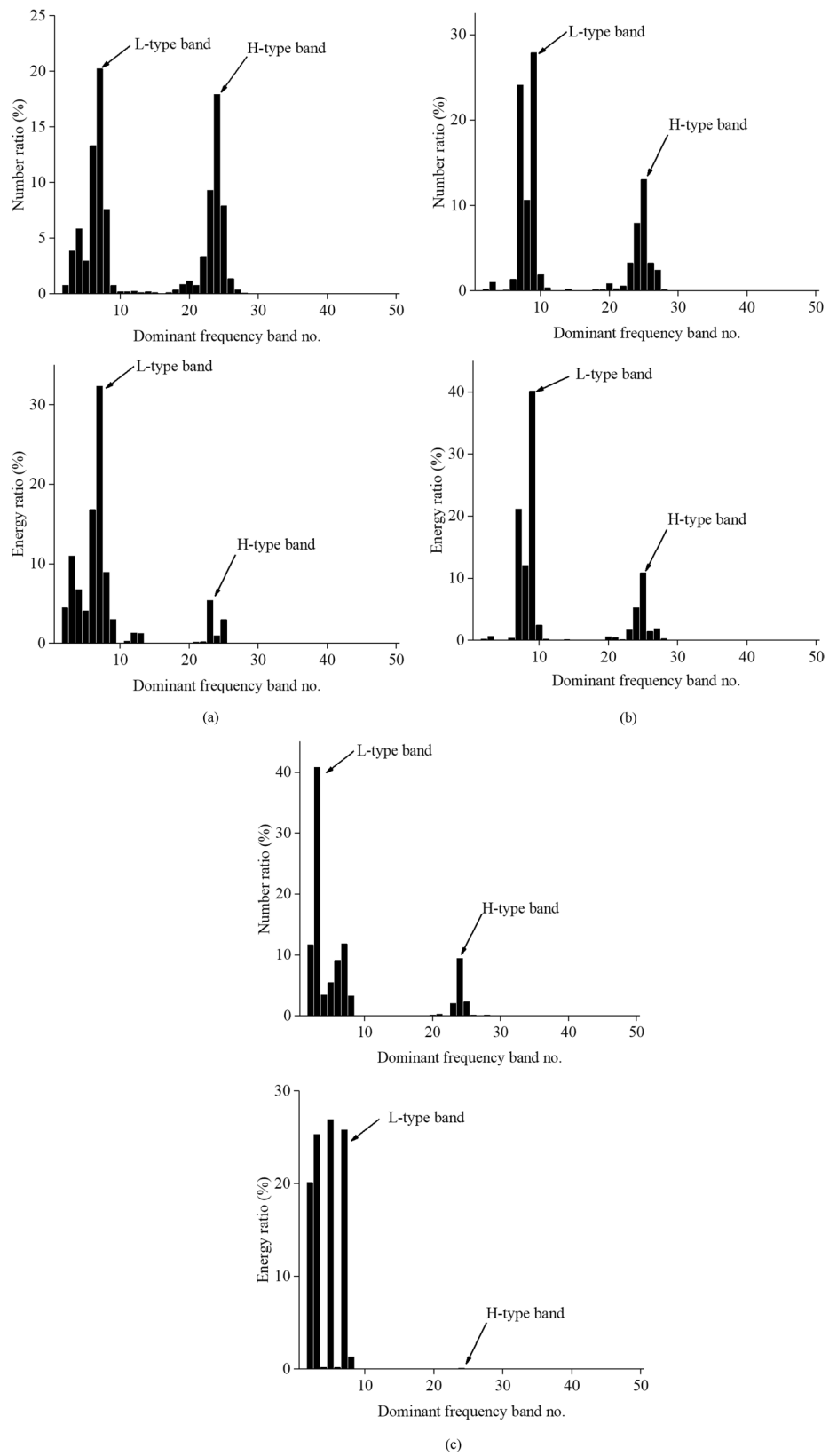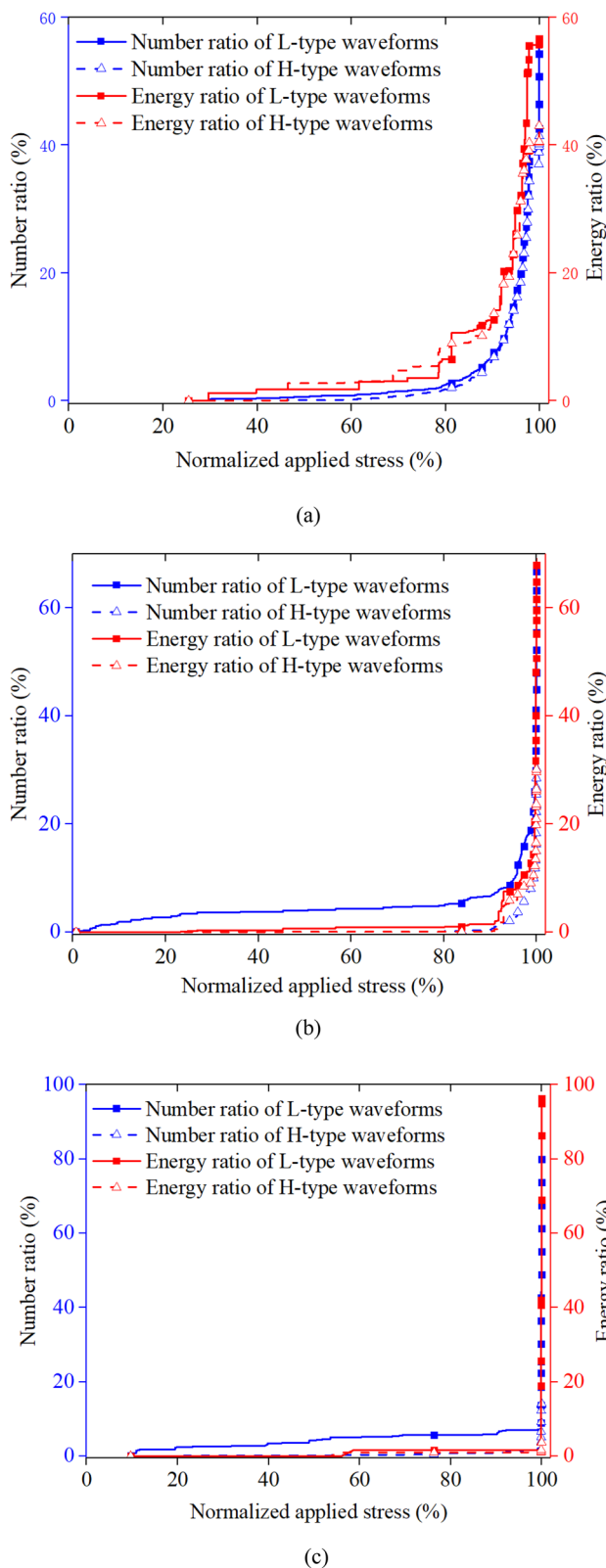

Fig. 6 Distribution characteristics of dominant frequencies of AE waveforms with normalized applied stress in rock samples: **a** granite; **b** basalt and **c** marble

Fig. 7 Statistical results of AE waveforms distributed in different dominant frequency bands according to number and energy: **a** granite; **b** basalt and **c** marble


(a)

(b)

(c)

(a)

(b)

(c)

Fig. 8 Cumulative curve of the proportions of L-type and H-type AE waveforms with the increasing normalized stress according to number and energy: **a** granite; **b** basalt and **c** marble

frequency band (L-type band) and high dominant frequency band (H-type band), which is consistent with the past findings (He et al. 2010; Li et al. 2017; Zhang et al. 2018). AE waveforms distributed in low and high dominant frequency bands are called L-type and H-type waveforms. Additionally, AE signals are released earlier in basalt specimens compared to granite and marble specimens. This can be attributed to the complex mineral composition and cementation type of basalt. Typical spatial distribution of L-type and H-type waveforms is shown in Fig. 3.

The dominant frequencies of AE waveforms were grouped into 50 bands for statistical analyses. The range of each band was set as 10 kHz, where the No. 1 band ranges from 0 to 10 kHz and the No. 50 band ranges from 490 to 500 kHz. AE signals were divided into different dominant frequency bands according to the magnitude of dominant frequencies. The number and energy statistics of AE waveforms in different dominant frequency bands were made. Statistical results of AE waveforms distributed in different dominant frequency bands according to number and energy are illustrated in Fig. 7. On average, the number ratios of L-type and H-type waveforms are 46.78% and 53.22% for granite, 71.41% and 28.59% for basalt, and 88.12% and 11.88% for marble. The energy of L-type waveforms accounts for 76.50% for granite, 89.95% for basalt and 99.80% for marble, while that of H-type waveform constitutes 23.50% for granite, 10.04% for basalt and 0.20% for marble, respectively. After comparing the proportions of L-type and H-type waveforms according to number and energy, energy ratios of L-type waveforms are greater than number ratios for each rock type, whereas energy ratios of H-type waveforms are less than the corresponding number ratios. That is, L-type waveforms of the same proportion carry more energy compared to H-type waveforms in rock subjected to tension.

### 3.3.3 Accumulation Law of L-Type and H-Type Waveforms with the Normalized Applied Stress

The normalized applied stress is defined as the ratio of the current stress to the peak strength of the rock sample. Cumulative curves of the proportions of L-type and H-type AE waveforms with the increasing normalized stress according to number and energy are shown in Fig. 8. It is found that the proportions of L-type and H-type waveforms both increase with the increasing stress level. There are less L-type and H-type waveforms at lower stress, but at higher stress level, especially when the stress is close to the peak strength, L-type and H-type waveforms grows significantly. Normalized applied stresses at the initial release moment of L-type and H-type waveforms were calculated to compare the release time sequence of L-type and H-type waveforms. Normalized applied stresses at the initial release moment
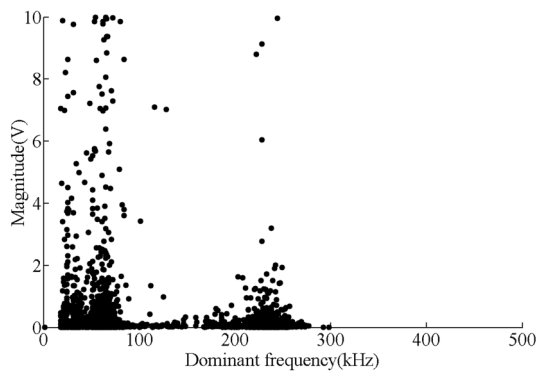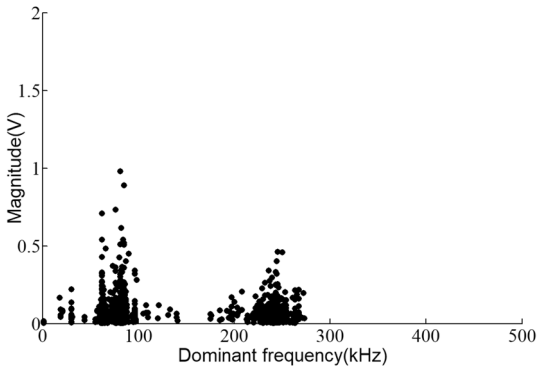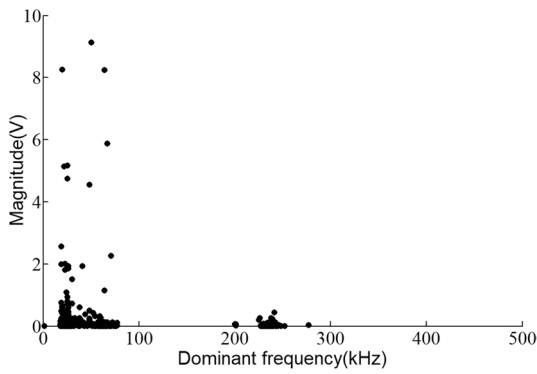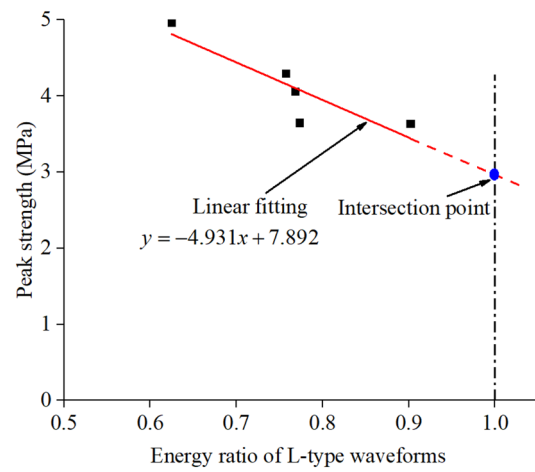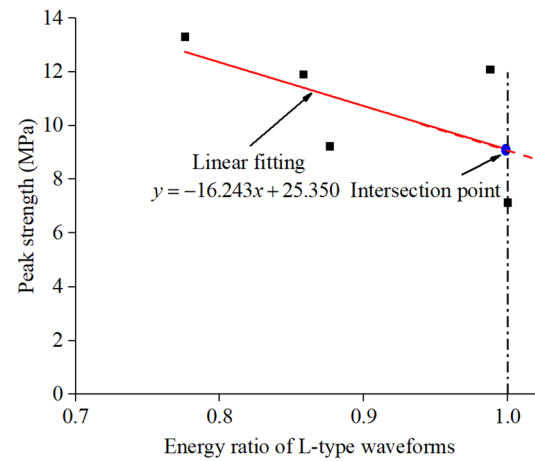
Fig. 9 Relationship between dominant frequency and amplitude of AE signals: **a** granite; **b** basalt and **c** marble
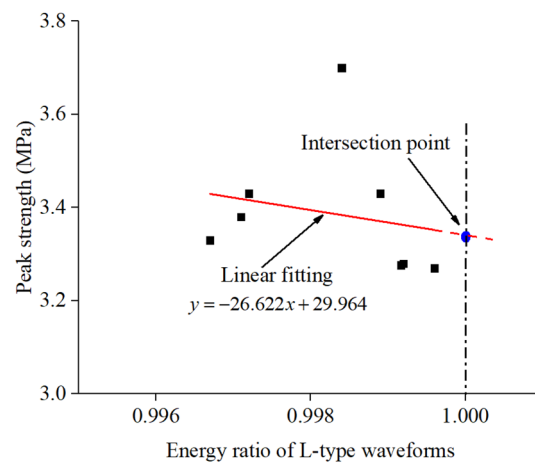
of L-type waveforms are averagely 13.39% for granite, 5.84% for basalt and 24.08% for marble, whereas those of H-type waveforms are 30.84% for granite, 31.81% for basalt, 48.07% for marble, respectively. Obviously, initial release moments of L-type waveforms appeared earlier than H-type waveforms.

Fig. 10 Relationship between peak strengths of rock and energy ratio of L-type waveforms: **a** granite; **b** basalt and **c** marble

3.3.4 Relationship Between Dominant Frequencies and Amplitude of AE Waveforms

Released energy is proportional to the square of amplitude of AE waveforms. Therefore, a study on the relationship between dominant frequency and amplitude can promote better understanding of AE signal characteristics of rock subjected to tension. Relationship between dominant frequency and amplitude of AE signals in common rocks is shown in Fig. 9. Although the large amplitude events of rock samples are distributed in both high and low dominant frequency bands, overall, there are obviously more large-amplitude events in the L-type band. This indicates the energy carried by H-type waveforms is significantly less than that of L-type waveforms.

3.4 Relationship Between Rock Tensile Strength and L-Type Waveforms

AE signals are produced by micro failures in rocks due to a rapid release of localized strain energy. Initiation, propagation and coalescence of micro failures result in the final macroscopic rock failure. Therefore, the energy of AE signals can better characterize rock failure characteristics than quantity. To discuss the correlation between dominant frequency characteristics of AE signals and tensile strength of rock, the statistical relationship between the energy ratios of L-type waveforms and peak strengths of rock specimens under tension was established. Taking the energy ratio of L-type waveforms as the abscissa and the peak strength of rock as the ordinate, a scatter plot was drawn (see Fig. 10). The black square data points in Fig. 10 represent the test results of rock specimens. Obviously, there is an overall downward trend for peak strength of rock specimens with the increasing energy ratios of L-type waveforms. A trend line for each rock was drawn by linear fitting. The linear fitting functions between the energy ratios of L-type waveforms (x) and peak strengths of rock specimens under tension (y) are for granite, basalt and marble as follows:

$$y = -4.9314x + 7.8918, \quad \text{for granite,} \tag{4}$$

Table 4 Natural frequencies of rock specimens

Rock type	Mass (kg)	Stiffness (MN/m)	Natural frequency (kHz)
Granite	0.51	472.05	4.82
Basalt	0.57	1415.68	7.91
Marble	0.53	448.44	4.65

$$y = -16.243x + 25.350, \quad \text{for basalt,} \tag{5}$$

$$y = -26.622x + 29.964, \quad \text{for marble.} \tag{6}$$

4 Discussion

Here we discussed the influence of natural frequencies of AE sensors and rock specimens on dominant frequency characteristics of AE signals. The natural frequency of Micro30 sensors is 200 kHz. It can be found from Figs. 6 and 7 that there is no aggregation phenomenon near 200 kHz in the dominant frequency of AE waveforms. Therefore, the natural frequency of AE sensors has no effect on the dominant frequency characteristics of AE waveforms. In addition, Micro30 sensors have a good frequency response in the range from 1 kHz to 1 MHz through sensitivity test. The sensitivity calibration curve of AE sensor can refer to Fig. 7 in our previous publication (Zhang and Deng 2020). Natural frequency of a solid is related to geometric dimensions and physical and mechanical properties. To calculate the natural frequency of rock specimens, a simplified formula of solid natural frequency (f) is introduced:

$$f = \frac{1}{2\pi}\sqrt{\frac{k}{m}}, \tag{7}$$

where the symbols k and m refer to the stiffness and mass of rock specimen.
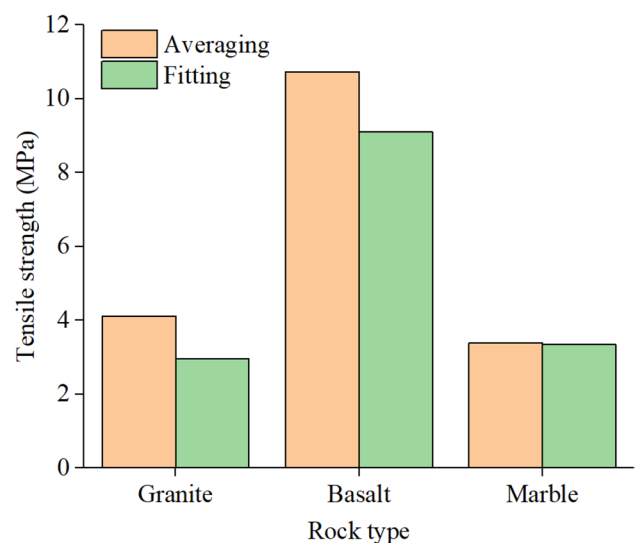
Fig. 11 Rock tensile strength acquired by the averaging and fitting methods

(a)

(b)

(c)
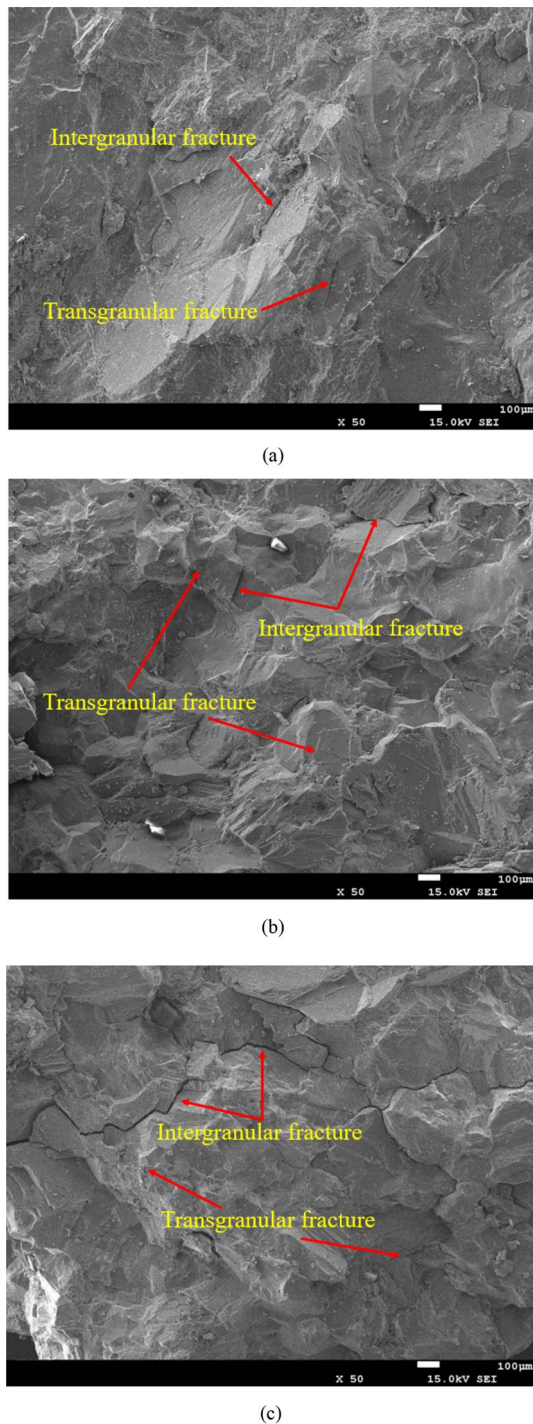
Fig. 12 SEM images of rock specimens after direct tensile failure: **a** granite; **b** basalt and **c** marble

Natural frequencies of each type of rock specimen were determined by Eq. (7). As listed in Table 4, natural frequencies of granite, basalt and marble specimens are 4.82, 7.91 and 4.65 kHz, respectively. Obviously, natural frequencies are below 10 kHz for rock specimens in this study. According to Figs. 6 and 7, there are very few AE waveforms whose

dominant frequencies are less than 10 kHz. Consequently, the dominant frequency characteristics of AE signals are not affected by the natural frequency of the rock.

Because H-type waveforms are generated by micro-shear failure and L-type waveforms are released by micro-tensile failure (Li et al. 2017; Zhang et al. 2018), the peak strength corresponding to the case that L-type waveforms (or micro tensile failures) account for 100% is considered as the "ideal" tensile strength from the microscopic perspective. The "ideal" tensile strength of rock corresponds to the strength at the intersection point between the outward extension line of the trend line and the vertical line whose energy ratio of L-type waveforms is 1 or 100% (see the blue dot in Fig. 10). The "ideal" tensile strengths by fitting are 2.96, 9.11 and 3.34 MPa for granite, basalt and marble, respectively. Furthermore, initial release moments of L-type waveforms appeared earlier than H-type waveforms (see Sect. 3.3.2), which implies micro tensile failure occurs earlier than micro shear failure.

Currently, the tensile strength of a rock is derived from the average of peak strengths of a set of rock specimens under tension. A comparison was made between tensile strengths of rock calculated by fitting and averaging, as shown in Fig. 11. Tensile strengths of granite, basalt and marble calculated by averaging are 4.12, 10.74 and 3.39 MPa compared to 2.96, 9.11 and 3.34 MPa for fitting, respectively. It can be found that the tensile strength of rock obtained by fitting in this study is smaller than that obtained by averaging. Therefore, the determined tensile strength by fitting can be used as a conservative design parameter for rock engineering, e.g., underground space development, shale gas production and tunnel excavation. In current engineering applications, tensile strength can be acquired by averaging the peak strengths of a set of rock samples. The fitting method proposed in this study involves spectrum analysis and dominant frequency statistics. The fitting method is time-consuming but more accurate compared with the averaging method. As a result, the averaging or fitting method can be selected for determining rock tensile strength according to actual needs, such as budget, time planning, and accuracy requirement.

To visually observe the microscopic failure patterns of rock, microstructural observations with SEM (scanning electron microscope) were further carried out. Figure 12 shows SEM images of rock specimens after direct tensile failure. Both intergranular and transgranular fractures exist in the process of rock tensile failure. Note that intergranular and transgranular fractures refer to micro fractures (or cracks) along the grain boundaries and within the grains. In addition, there exist micropores or convex bodies due to tensile loading. The identification of microscopic tensile or shear failure modes is mainly based on the morphology of fracture surface. Most of microscopic fractures can be classified as tensile failures because the fracture surfaces are curved,

rough and usually open. Some microscopic fracture surfaces are smooth and nearly linear, which can be judged as a shear failure. This indicates there exist micro shear failures during the macro tensile failure process of rock. Therefore, there is no complete tensile failure in the current test method at a microscopic scale. Even if the rock shows a tensile failure on a macroscopic level, it may contain shear or mixed failure on a microscopic level. The findings in this paper facilitate better understanding of rock tensile properties at a microscopic scale.

This study focuses on the evolution process of microcracks in rock under tension and the relationship between the energy ratios of AE waveforms distributed in different dominant frequency bands and peak strengths of a group of rock samples using the newly introduced quantitative analysis of AE waveforms. Granite, basalt and marble were used in this study. It is worth studying in more types of rocks. Besides, it is also worth to investigate further effects of water content and porosity. The topic could contribute to some interesting developments of future research.

5 Conclusions

In this study, a detailed micro analysis of rock direct tensile failure was made based on a statistical analysis of AE waveforms. The following conclusions can be drawn:

1. Mineral composition of rock poses an obvious effect on macro failure behaviors of rock. The dispersion degree of rock tensile strength corresponds well to the complexity of mineral composition.
2. There are two concentrations of dominant frequency bands during the direct tensile failure process of rock. The dominant frequency characteristics of AE signals are not affected by the natural frequencies of the rock and AE sensor. Initial release moments of L-type waveforms appeared earlier than H-type waveforms. L-type waveforms of the same proportion carry more energy compared to H-type waveforms in rock subjected to tension.
3. There is an overall downward trend for peak strength of rock specimens with the increasing energy ratios of L-type waveforms. The tensile strength of rock obtained by fitting is smaller than that obtained by averaging. The peak strength corresponding to the case that L-type waveforms (or micro tensile failures) account for 100% can be considered as the "ideal" tensile strength from the microscopic perspective. The determined tensile strength by fitting can be used as a conservative design parameter for rock engineering.
4. There exist micro shear fractures during the macro tensile failure process of rock according to the micro-

structural observations with SEM. There is no complete tensile failure in the current test method at a microscopic scale.

Declarations

Conflict of interest The authors declare that they have no conflicts of interest.

References

Aker E, Kühn D, Vavryčuk V, Soldal M, Oye V (2014) Experimental investigation of acoustic emissions and their moment tensors in rock during failure. Int J Rock Mech Min Sci 70:286–295

Cai M, Morioka H, Kaiser PK, Tasaka Y, Kurose H, Minami M, Maejima T (2007) Back-analysis of rock mass strength parameters using AE monitoring data. Int J Rock Mech Min Sci 44(4):538–549

Dan DQ, Konietzky H, Herbst M (2013) Brazilian tensile strength tests on some anisotropic rocks. Int J Rock Mech Min Sci 58:1–7

Diederichs MS, Kaiser PK (1999) Tensile strength and abutment relaxation as failure control mechanisms in underground excavations. Int J Rock Mech Min Sci 36(1):69–96

Du K, Li X, Tao M, Wang S (2020) Experimental study on acoustic emission (AE) characteristics and crack classification during rock fracture in several basic lab tests. Int J Rock Mech Min Sci 133:104411

Fahimifar A, Malekpour M (2012) Experimental and numerical analysis of indirect and direct tensile strength using fracture mechanics concepts. B Eng Geol Environ 71(2):269–283

Goodman RE (1989) Introduction to rock mechanics. Wiley, New York

Grosse CU, Ohtsu M (eds) (2008) Acoustic emission testing. Springer, Berlin

He MC, Miao JL, Feng JL (2010) Rock burst process of limestone and its acoustic emission characteristics under true-triaxial unloading conditions. Int J Rock Mech Min Sci 47(2):286–298

Hobbs DW (1967) Rock tensile strength and its relationship to a number of alternative measures of rock strength. Int J Rock Mech Min Sci Geomech Abstr 4(1):115–127

Huang Y, Deng J, Zhu J (2019) An experimental investigation of moisture-induced softening mechanism of marble based on quantitative analysis of acoustic emission waveforms. Appl Sci 9:446

Ishiguro S, Nakaya M (1985) Direct tensile strength of steel fiber reinforced concrete by using clamping grips. Bull Univ Osaka Prefect Ser B Agric Biol Osaka (prefect) Daigaku 37:69–73

ISRM (1978) Suggested methods for determining tensile strength of rock materials. Int J Rock Mech Min Sci Geomech Abstr 15(3):99–103

Karser J (1950) A study of acoustic emission phenomena in tensile tests. PhD thesis. FRG: Technische Hochschule Munchen

Li LR, Deng JH, Zheng L, Liu JF (2017) Dominant frequency characteristics of acoustic emissions in white marble during direct tensile tests. Rock Mech Rock Eng 50(5):1337–1346

Liang Z, Xue R, Xu N, Li W (2020) Characterizing rockbursts and analysis on frequency-spectrum evolutionary law of rockburst precursor based on microseismic monitoring. Tunn Undergr Sp Tech 105:103564

Liao JJ, Yang MT, Hsieh HY (1997) Direct tensile behavior of a transversely isotropic rock. Int J Rock Mech Min Sci 34:837–849

Perras MA, Diederichs MS (2014) A review of the tensile strength of rock: concepts and testing. Geotech Geol Eng 32:525–546

Shiotani T, Ohtsu M, Ikeda K (2001) Detection and evaluation of AE waves due to rock deformation. Constr Build Mater 15(5):235–246

Sondergeld CH, Estey LH (1981) Acoustic emission study of microfracturing during the cyclic loading of Westerly granite. J Geophys Res Solid Earth 86(B4):2915–2924

Toutanji HA, Liu L, El-Korchi T (1999) The role of silica fume in the direct tensile strength of cement-based materials. Mater Struct 32(3):203–209

Wijk G, Rehbinder G, Lögdström G (1978) The relation between the uniaxial tensile strength and the sample size for bohus granite. Rock Mech 10(4):201–219

Wu C, Chen X, Hong Y, Xu R, Yu D (2018) Experimental investigation of the tensile behavior of rock with fully grouted bolts by the direct tensile test. Rock Mech Rock Eng 51:351–357

Zhang ZH, Deng JH (2020) A new method for determining the crack classification criterion in acoustic emission parameter analysis. Int J Rock Mech Min Sci 130:104323

Zhang ZH, Deng JH, Zhu JB, Li LR (2018) An experimental investigation of the failure mechanisms of jointed and intact marble under compression based on quantitative analysis of acoustic emission waveforms. Rock Mech Rock Eng 51(7):2299–2307

Zhang ZH, Li YC, Hu LH, Tang CA, Zheng HC (2020) Predicting rock failure with the critical slowing down theory. Eng Geol 280:105960

Zhou H, Meng F, Zhang C, Hu D, Lu J, Xu R (2016) Investigation of the acoustic emission characteristics of artificial saw-tooth joints under shearing condition. Acta Geotech 11(4):925–939